

**COB-2023-0570**

## **EXPERIMENTAL INVESTIGATION OF WATER-MEG MIXING IN A HELE-SHAW CELL WITH CHANGE OF DIRECTION**

**Pedro Leineker Ochoski Machado**

**Anna Carolina Zornitta Liston**

**Leonardo Pereira França de Souza**

**Elcilane Araujo de Freitas**

**Moisés Alves Marcelino Neto**

**Rigoberto E. M. Morales**

Multiphase Flow Research Center – NUEM, Graduate Program in Mechanical and Materials Engineering – PPGEM, Federal University of Technology – Paraná, 5000 Deputado Heitor Alencar Furtado Street, Curitiba, PR, Brazil.  
pedmac@alunos.utfpr.edu.br, annaliston@alunos.utfpr.edu.br, leonardosouza.2020@alunos.utfpr.edu.br, elcilanef@alunos.utfpr.edu.br, mneto@utfpr.edu.br, rmorales@utfpr.edu.br

**Joel Robert Karp**

CORIA, University of Rouen, Madrillet University Site, 675 University Avenue, Saint Etienne, France.  
karp.joelr@gmail.com

**Amadeu K. Sum**

Colorado School of Mines, 1500 Illinois St., Golden, Colorado, USA.

**Abstract.** *The formation of hydrates is often observed after unplanned shutdowns in the petroleum production lines, representing a significant threat to the operation as they can agglomerate and cause either partial or total blockage of the pipeline. The presence of water, oil and gas in the pipeline, plus to the low temperatures and high pressures related to the restart of the operation, provokes the formation of these compounds. It then becomes necessary to use strategies that inhibit their formation such as the injection of thermodynamic inhibitors, which change the hydrate formation curve when mixed with water. Despite their wide application, the mixing of thermodynamic inhibitors such as MEG (monoethylene glycol), with water is not fully understood, as there is a lack of studies about the water-MEG mixing in the literature. Thus, this work proposes to investigate the water-MEG mixing experimentally. To this end, experiments are conducted in a transparent Hele-Shaw test section (6-mm gap between flat plates) with different flow orientations (vertical and horizontal), thus enabling the visual monitoring of the mixing process. MEG was injected into quiescent water in the test section at different locations, with different injection directions (perpendicular and coaxial with the flow direction), different flow rates and different concentrations, resulting in different Reynolds ( $Re$ ), Atwood ( $At$ ), and Froude ( $Fr$ ) numbers. Samples were collected and analyzed via a HANNA® instruments Digital Refractometer for Ethylene Glycol Analysis HI96831. The experimental results showed that the injection methodology greatly affects the mixing since proper mixing is easily achieved by vertical injection, and poor mixing is obtained by injection in a horizontal section mostly due to buoyant forces resulting from the density difference (MEG is heavier than water). To improve the mixing in a horizontal section, diluted MEG and higher flow rates can be used.*

**Keywords:** *thermodynamic inhibitor, mixing, water-MEG mixing, hydrate inhibitor*

### **1. INTRODUCTION**

Aiming to meet the growing global energy demands, the energy sector is in constant search of new energy exploration strategies, either from alternative sources or from the adaptation of existing processes. The increasing depths in the offshore exploration of oil and gas (Najibi et al., 2022) is an example.

In such circumstances, the formation of gas hydrates is likely to occur, as oil, water and gas are found at high-pressure and low-temperature conditions, while unplanned shutdowns and the increase of water content in the pipeline may also contribute to the hydrate formation (Aminnaji et al., 2017).

The hydrate particles may adhere and agglomerate into flow lines, valves and instruments, causing the partial or full blockage of a pipeline. This is one of the main flow assurance issues in oil and gas exploitation processes given its fast formation rate, causing production impairment or stoppage and other safety and economic threats (AlHarooni et al., 2015; Wang et al., 2019).

Since the removal of the hydrate plugs is very challenging, expensive and worrisome from a safety standpoint, the main approach to deal with hydrates in production pipelines is their avoidance, based on pipeline temperature control,

depressurization or continuous injection of thermodynamic hydrate inhibitors (THIs) (Burgass et al., 2018; Wang et al., 2019).

Methanol (CH<sub>3</sub>OH) and/or monoethylene glycol (MEG) act as THIs when injected into the pipeline, degrading pre-existing hydrate particles and inhibiting further hydrate formation. The inhibition process occurs because of its ability to shift the phase-equilibrium conditions in such a way that higher pressures and lower temperatures would be required for the hydrates to be formed (Aminnaji et al., 2017). MEG is found to be more suitable for pipeline injection than methanol due to its chemical stability, lesser environmental effects, low solubility with final gas products and high regeneration efficiency (Alef et al., 2018).

Table 1 shows the main dimensionless numbers related to the injection of a fluid into another, in which  $\rho$  is the fluid density and  $\mu$  its viscosity, while the subscript  $i$  corresponds to the injected fluid and  $q$  to the quiescent one.  $D$  and  $d$  represent the main pipe and the injection pipe diameters, respectively, while  $v$  is the injection velocity in the injection pipe,  $V$  is the velocity in the main pipe,  $L$  is the main pipe length and  $g$  is the gravity acceleration. The binary molecular diffusion coefficient is given by  $D_m$ .

Table 1. Dimensionless numbers related to the injection of a fluid into another (Akbari and Taghavi, 2020).

Dimensionless number	Definition
Reynolds – $Re$	$Re = \frac{\rho_i v d}{\mu_i}$
Atwood – $At$	$At = \frac{\rho_i - \rho_q}{\rho_i + \rho_q}$
Froude – $Fr$	$Fr = \frac{V}{\sqrt{Atgd}}$
Peclet – $Pe$	$Pe = \frac{VD}{D_m}$
Slope - $\beta$	From horizontal
Aspect ratio - $\delta$	$\delta = \frac{L}{D}$
Diameter ratio – $D_r$	$D_r = \frac{d}{D}$
Viscosity Ratio - $m$	$m = \frac{\mu_q}{\mu_i}$

Regarding fluid displacement/mixing studies in the literature, it was shown that as the flow tends to the vertical downward (inertia and buoyancy acting in the same direction), the instabilities and the mixing between the fluids increase (Sahu et al., 2009; Alba et al., 2013; Akbari and Taghavi, 2020). In the case of a  $D_r = 1$ , it was verified that as the Reynolds number increases, the mixing and instabilities between the fluids decrease (Amiri et al., 2016), while for  $D_r < 1$  it was shown that the turbulence and mixing between the fluids in the transverse direction of the flow increase when  $Re$  increases (Akbari and Taghavi, 2020), as the flow energy dissipation closer to the injection point is higher for lower  $Re$  (Hassanzadeh et al., 2021).

In general, reducing  $Fr$  resulted in a better mixing between the fluids (Alba et al., 2013; Akbari and Taghavi, 2020), which was also observed when increasing  $At$  in vertical flows (Amiri et al., 2016). A reduction in the viscosity ratio resulted in a lower amount of mixing and instabilities between the fluids (Erati et al., 2018; Akbari and Taghavi, 2021).

There is a lack of studies in the literature regarding the mixing process of MEG in water or multi-component mixture. As pointed out by Karami et al. (2017), the MEG mixing in multiphase flow and its effects on flow parameters are not well understood. To the best of our knowledge, an optimized injection methodology, e.g., injection rate, angle, and location of the injection has yet to be presented. The pioneer study on THIs mixing was performed by Valim (2018). Using experimental and numerical procedures, the mixing of MEG and/or ethanol in quiescent water was analyzed in a vertical and tilted column (4°). Although infinitely miscible in water, the mixing in the water of those THIs behaves differently. Even for higher injection rates, MEG tends to accumulate at the bottom of the column, whereas ethanol showed a more uniform concentration along the column. For the inclined configuration, higher ethanol concentrations were found at the top of the test section.

Based on the literature review shown above, the present study aims to experimentally verify the influence of flow parameters in the water-MEG mixing in a thin gap with change in direction, namely the injection rate, concentration, angle and injection location.

## 2. METHODOLOGY

This section presents the apparatus and procedures used to achieve the main goal of this work.

## 2.1 Experimental apparatus

The test section is presented in Fig. 1. (a) and (b). It was composed of a transparent Hele-Shaw cell with changes of direction with three regions, two vertical columns and a horizontal one. The flow channels were made of 6-mm wide glass sheets, resulting in a hydraulic diameter of approximately 10.7 mm. The exterior was made of polyoxymethylene sheets, on which 6-mm quick-connect couplings were placed in different positions to allow fluid injection, as shown in Fig. 1 (a).

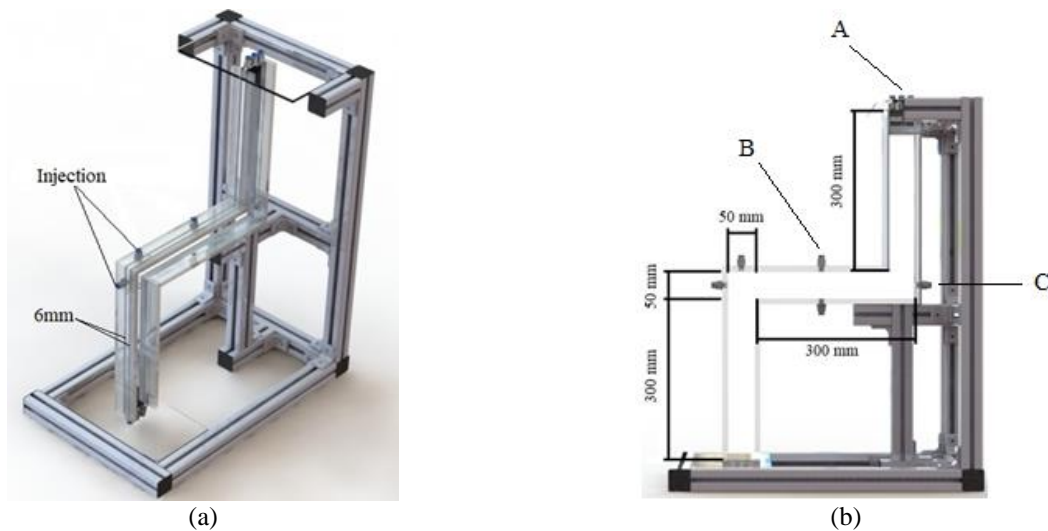


Figure 1. Test section: (a) Isometric view; (b) Dimensions.

## 2.2 Experimental procedure

To assess the mixing of water and MEG the test section was, at first, completely filled with water. Two different injection methods were used, one with a 3-mm injection tube and another with a tube with an internal diameter of 1.5 mm, resulting in diameter ratios of 0.28 and 0.14, respectively. Three different injection points were selected and designated as A, B, and C, according to Fig. 1 (b). The first is co-axial at the top of the test section ( $A - \beta = 90^\circ$ ); the second is perpendicular to the horizontal section ( $B - \beta = 90^\circ$ ), and the third is co-axial at the horizontal section ( $C - \beta = 0^\circ$ ). Two different inlet MEG concentrations ( $C_i$  %v/v) were used, pure MEG ( $C_i = 100$  %v/v) and diluted MEG ( $C_i = 70$  %v/v).

For every experimental point, the test section was at first completely filled with tap water. To perform the MEG injection, a Teledyne<sup>TM</sup> 260D syringe pump was connected to the test section at the injection points. All the experiments were carried out in a condition in which a 20% v/v global concentration of MEG was found inside the test section. The temperature of the fluids and ambient was kept at 20°C, and orange dye (alcohol aniline) was added to the MEG in a proportion of 0.1 g/l for visualization purposes. Since the experiments were carried out in an overflow condition, two drains were placed at the top of the test section, at the side of injection point A.

Eight main sampling locations were used to perform MEG concentration measurements at each condition, three at each vertical section, and two at the horizontal one, as it can be seen in Fig. 2. At each sampling site, three samples were collected at different positions in the fluid channel, allowing a concentration gradient analysis at each location. During the fluid injection, the syringes were kept outside the flow channel, being only introduced to the sampling location 5 min after the injection was finished.

Table 2 summarizes the conditions used for the experiments. The concentration analyses of the samples were made by a HANNA<sup>®</sup> instruments Digital Refractometer for Ethylene Glycol Analysis HI96831, providing instantaneous MEG volumetric concentrations with automatic temperature correction and 0.4% v/v of uncertainty.

The injection results were evaluated in terms of the MEG concentration standard deviation ( $\sigma$ ) along the test section, and the influence of each injection parameter was evaluated through a correlation matrix using Pearson's Linear Correlation Coefficient at Matlab<sup>®</sup>.

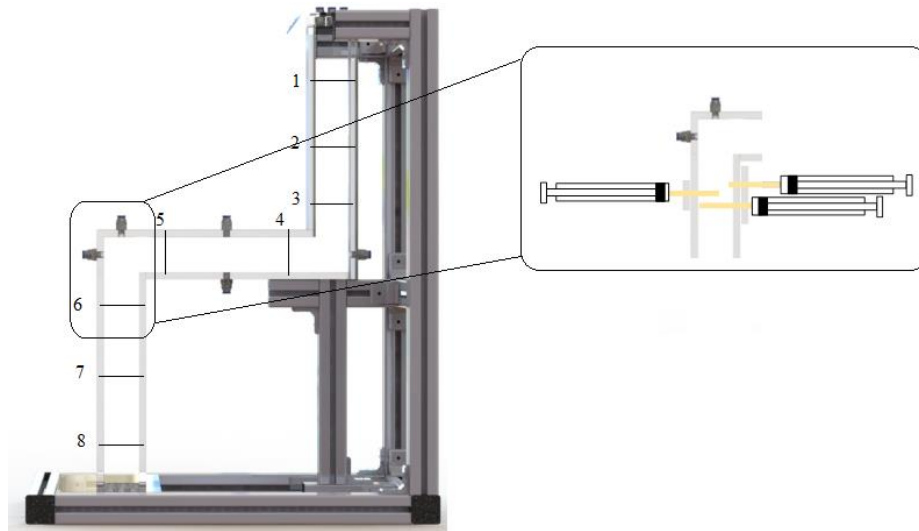


Figure 2. Sampling points.

Table 2. Experimental test matrix.

Experiment	$C_i$ [%v/v]	$C_g$ [%v/v]	Injection Position	Re	$D_r$	At	Fr	m
1	100			37.53	0.2804	0.0544	0.245	0.048
2	100			18.77	0.2804	0.0544	0.122	0.048
3	100			37.53	0.1402	0.0544	0.122	0.048
4	100			18.77	0.1402	0.0544	0.061	0.048
5	70		A	37.53	0.2804	0.0478	0.095	0.133
6	70		A	18.77	0.2804	0.0478	0.048	0.133
7	70		A	37.53	0.1402	0.0478	0.048	0.133
8	70		A	18.77	0.1402	0.0478	0.024	0.133
9	100			37.53	0.2804	0.0544	0.245	0.048
10	100			18.77	0.2804	0.0544	0.122	0.048
11	100			37.53	0.1402	0.0544	0.122	0.048
12	100			18.77	0.1402	0.0544	0.061	0.048
13	70	20	B	37.53	0.2804	0.0478	0.095	0.133
14	70	20	B	18.77	0.2804	0.0478	0.048	0.133
15	70	20	B	37.53	0.1402	0.0478	0.048	0.133
16	70	20	B	18.77	0.1402	0.0478	0.024	0.133
17	100			37.53	0.2804	0.0544	0.245	0.048
18	100			18.77	0.2804	0.0544	0.122	0.048
19	100			37.53	0.1402	0.0544	0.122	0.048
20	100			18.77	0.1402	0.0544	0.061	0.048
21	70		C	37.53	0.2804	0.0478	0.095	0.133
22	70		C	18.77	0.2804	0.0478	0.048	0.133
23	70		C	37.53	0.1402	0.0478	0.048	0.133
24	70		C	18.77	0.1402	0.0478	0.024	0.133

### 3. RESULTS

We begin by examining the influence of the injection location. Figure 3 displays the results obtained from Exp. 1 (a), Exp. 14 (b), and Exp. 18 (c), illustrating that injection from the top (injection point A) resulted in effective mixing, as indicated by the homogeneous color distribution throughout the entire test section. In contrast, poor mixing is observed for the middle injection point, where MEG exhibits a higher concentration at the bottom and in the middle, as suggested by the color gradient shown in Fig. 3 (b) and (c). Injection point C yielded the least favorable results among all three injection locations, with no MEG found in the top vertical region of the geometry.

This phenomenon arises due to the density difference between MEG and water. When a liquid flows over another liquid with differing densities, and both are miscible, a sharp density discontinuity interface can be observed. As the relative velocity between the fluids increases, waves start to form at the interface until a critical velocity is reached,

resulting in the mixing of the fluids due to the formation of periodically ejected eddies from the crest of the waves (Keulegan, 1949).

In the case of a positively buoyant jet directed downward, two flow regimes can be observed: semi-turbulent and turbulent. At low Reynolds numbers ( $Re$ ), the semi-turbulent regime features a laminar region near the fluid inlet, followed by jet collapse (turbulent region), where fluid mixing occurs (Hassanzadeh et al., 2021).

Jet collapse can occur due to Rayleigh-Taylor and Kelvin-Helmholtz instabilities. When MEG is injected from the top, instabilities form in the vertical section due to the density and velocity difference between the fluids, facilitating effective mixing. In the case of MEG injection at location B, where the flow channel is limited, there is minimal room for the jet to collapse, resulting in poor mixing. Regarding injection location C, since MEG is denser than water, buoyancy causes MEG to sink to the bottom of the flow channel, flowing beneath the layer of water and resulting in very poor mixing between the fluids.

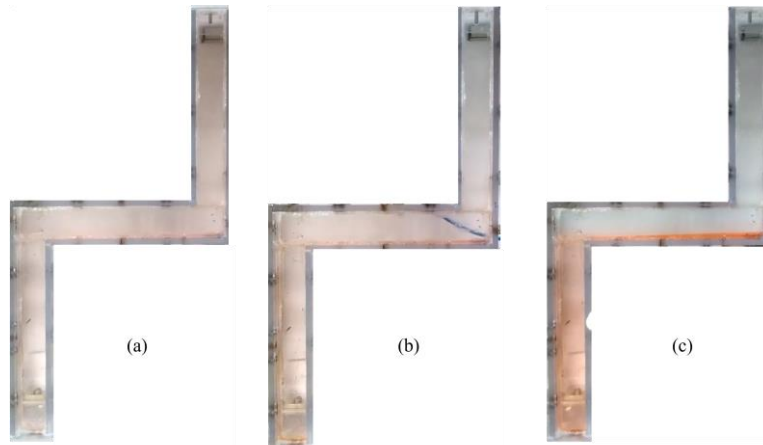


Figure 3. Results: (a) Experiment 1; (b) Experiment 14; (c) Experiment 18.

This can be further validated by analyzing the standard deviation of MEG concentration along the test section for each injection location. From Fig. 4, it is evident that the experimental points with the lowest standard deviation values were those obtained through injection point A, followed by injection point B, and finally, injection point C. Experimental points sharing the same symbol in Fig. 4 are those with the same injection conditions, except for the injection location. The highest relative difference from the average MEG concentration to the  $C_g$  (global concentration) was observed in the experimental points that used injection location A. This is due to the injection's proximity to the drain location, causing a higher amount of MEG to exit the geometry along with the overflow water.

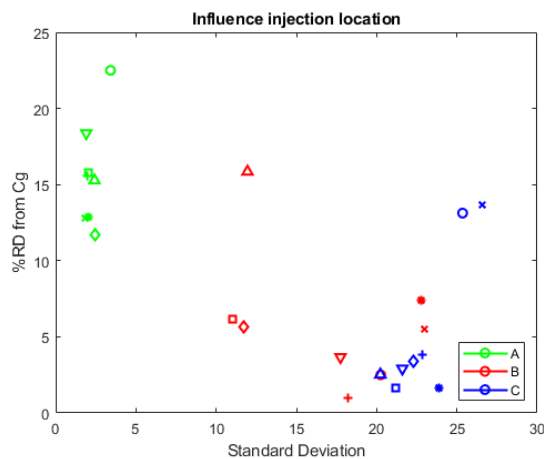


Figure 4. Influence of injection location on MEG distribution.

Fig. 5 (a), (b), and (c) present the results for experimental points 1 – 8 in terms of  $Re$ ,  $D_r$ , and  $C_i$ , respectively. In each figure, experimental points with the same symbols share the same injection parameters, except for the one being analyzed. In Fig. 5 (a), it is evident that, in general, lower  $Re$  values correspond to lower standard deviation values, a pattern

consistent with Fig. 5 (b) for the diameter ratio. Fig. 5 (c) shows that, when injecting MEG from the top downward, injecting pure MEG results in better mixing than injecting diluted MEG.

This observation is further supported by the correlation matrix presented in Fig. 6. The parameters that exert a substantial influence on mixing efficiency in this condition are  $Fr$ ,  $Re$ , and  $D_r$ , with their influence being directly proportional, as indicated by the positive correlation coefficient. In contrast,  $C_i$ ,  $At$ , and  $m$  exhibit low correlations with mixing efficiency because they have opposing effects on mixing in this injection direction. Reducing  $C_i$  increases  $m$ , promoting more instabilities at the fluid interface (Erati et al., 2018; Akbari and Taghavi, 2021). However, reducing  $C_i$  also decreases  $At$ , which has the opposite effect (Amiri et al., 2016). Thus, the effect of  $m$  is mitigated by the counter-effect promoted by  $At$ .

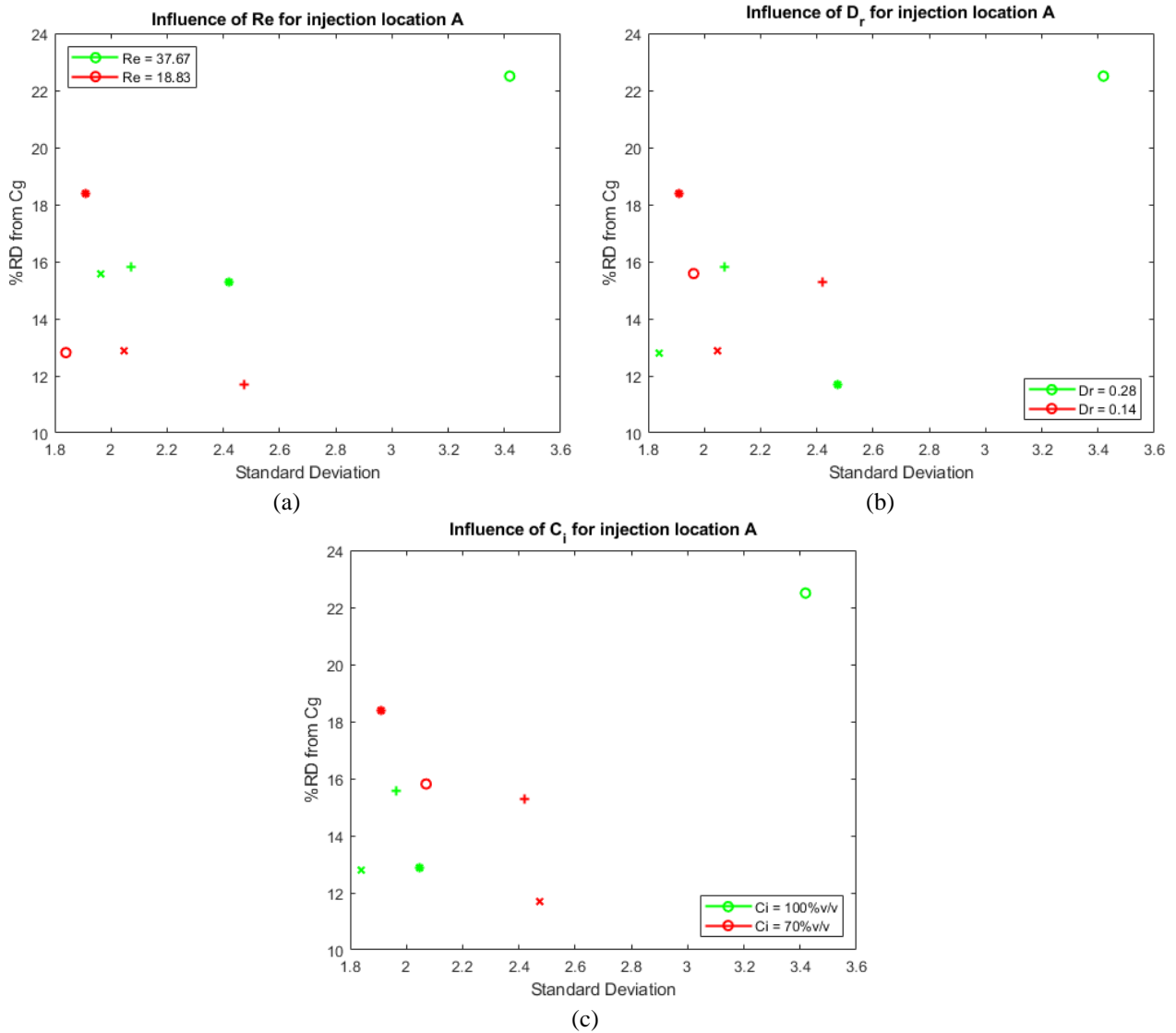


Figure 5. Injection Location A. (a) Influence of  $Re$ ; (b) Influence of  $D_r$ ; (c) Influence of  $C_i$ .

Fig. 7 (a), (b), and (c) reveal the results for experimental points 9 – 16 in terms of  $Re$ ,  $D_r$ , and  $C_i$ , respectively. In Fig. 7 (a), it can be observed that, in general, higher  $Re$  values correspond to lower standard deviation values, which is opposite to the trend observed for the diameter ratio in Fig. 7 (b). In Fig. 7 (c), it is clear that injecting diluted MEG results in better mixing than injecting pure MEG.

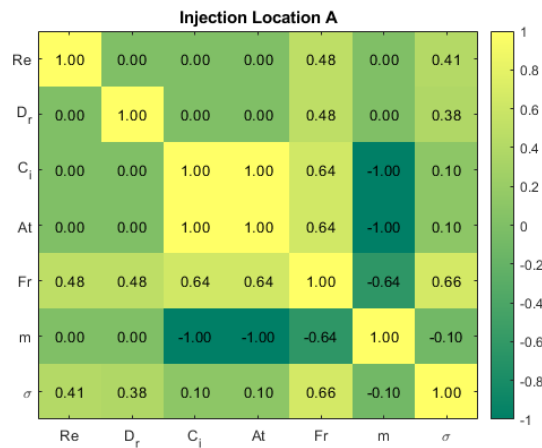


Figure 6. Correlation matrix for Injection Location A.

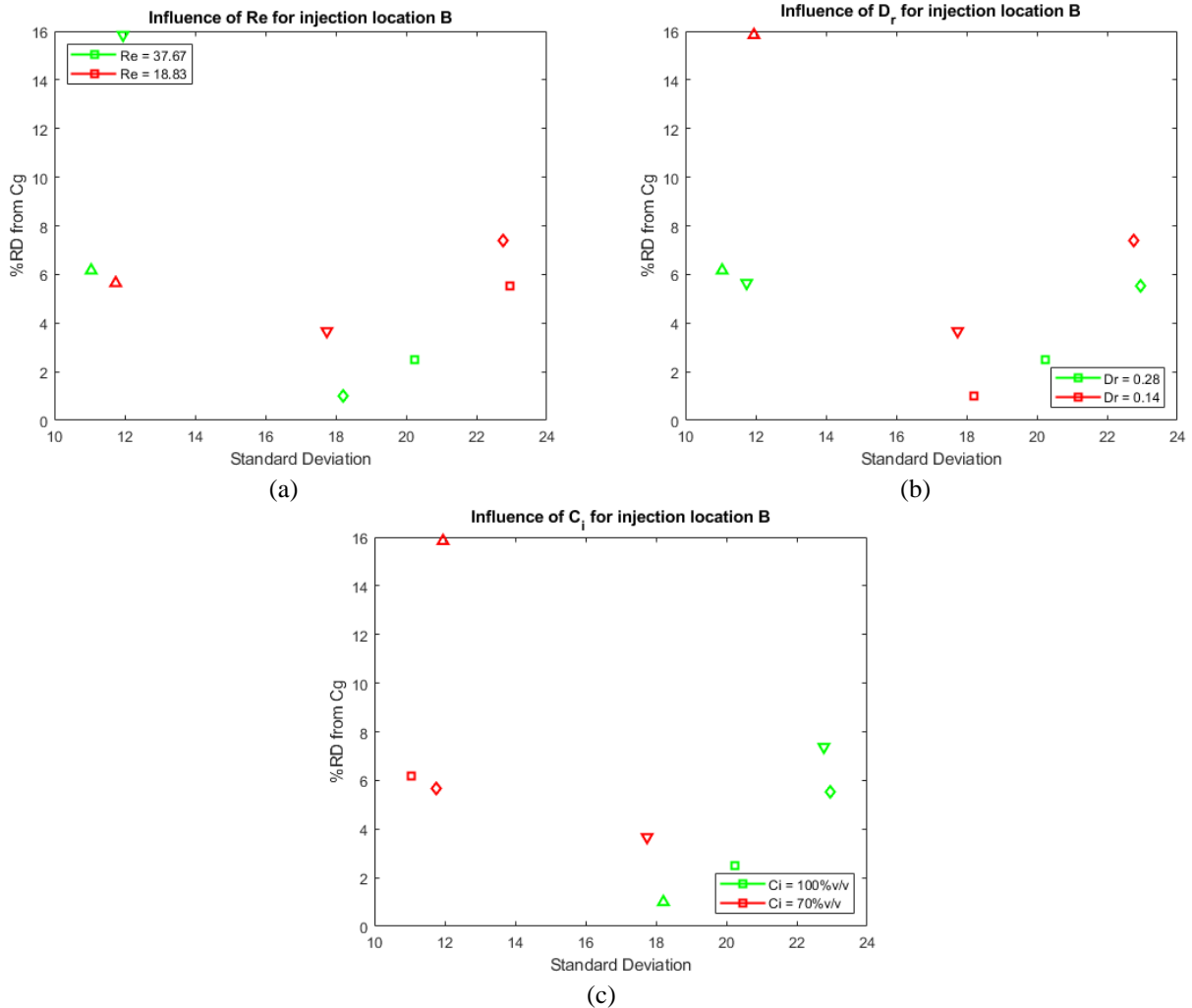


Figure 7. Injection Location B. (a) Influence of  $Re$ ; (b) Influence of  $D_r$ ; (c) Influence of  $C_i$ .

Fig. 8 demonstrates that the impact of dilution is more pronounced on the standard deviation result at injection location B than at injection location A. Parameters  $C_i$  and  $At$  exhibit a very strong positive correlation, indicating that lower values of  $C_i$  and  $At$  result in lower standard deviation values. Additionally, the viscosity ratio exhibits a very strong negative correlation, signifying that increasing  $m$  decreases  $\sigma$ . These findings are in line with existing literature, as increasing  $At$  in a horizontal section tends to promote fluid stratification while raising  $m$  and lowering  $Fr$  generates instabilities at the fluid interface. Decreasing  $Fr$  also reduces  $\sigma$ , whereas reducing  $Re$  and  $D_r$  increases  $\sigma$ .

Fig. 9 (a), (b), and (c) show the results for experimental points 17 – 24 in terms of  $Re$ ,  $D_r$ , and  $C_i$ , respectively. In Fig. 9 (a), it is clear that, in general, higher  $Re$  values correspond to lower standard deviation values, the opposite of what was observed for the diameter ratio in Fig. 9 (b). Fig. 9 (c) shows that injecting diluted MEG results in better mixing than injecting pure MEG.



Figure 8. Correlation matrix for Injection Location B.

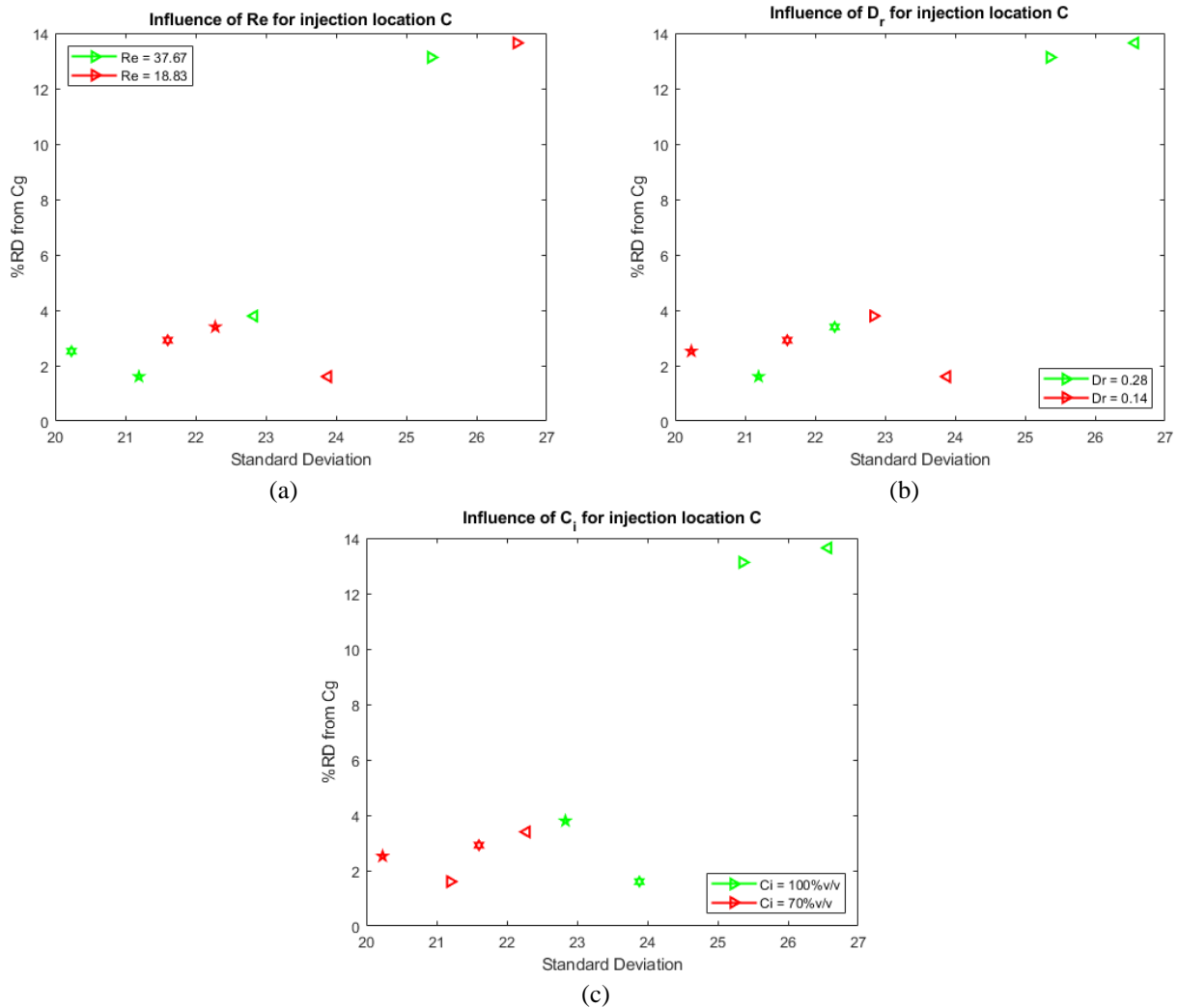


Figure 9. Injection Location C. (a) Influence of  $Re$ ; (b) Influence of  $D_r$ ; (c) Influence of  $C_i$ .

Furthermore, from Fig. 10, it can be observed that the impact of dilution is also more significant on the standard deviation result at injection location C than at injection location A.

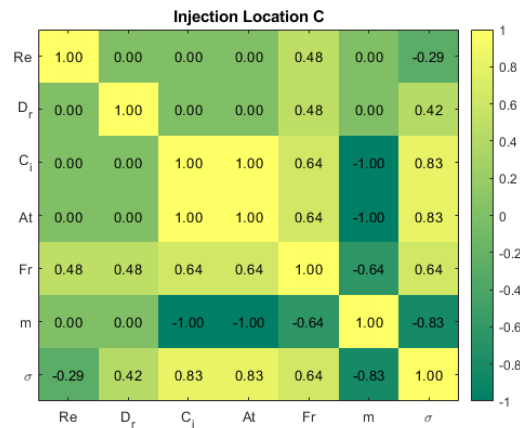


Figure 10. Correlation matrix for Injection Location C.

#### 4. CONCLUSIONS

In this study, we investigated the influence of various injection parameters on the mixing of water and MEG within a Hele-Shaw test section with changes in direction. Our experiments revealed several important insights:

- The choice of injection methodology significantly impacts the mixing efficiency. Vertical injection tends to yield effective mixing, while horizontal injection in a Hele-Shaw test section results in poor mixing.
- We found that injection location plays a crucial role in determining the efficiency of MEG-water mixing. Different parameters have varying effects on the mixing process at each location.
- In the case of vertical downward injection, parameters such as Reynolds number ( $Re$ ), Froude number ( $Fr$ ), and diameter ratio ( $D_r$ ) were identified as key factors influencing proper mixing. Their reduction correlated with a decrease in the standard deviation of MEG concentration, indicating improved mixing.
- For horizontal injection perpendicular to the flow direction, fluid inlet concentration ( $C_i$ ) emerged as the primary parameter affecting mixing. Dilution before injection led to a reduction in Atwood number ( $At$ ) and an increase in the viscosity ratio ( $m$ ), resulting in a lower standard deviation for MEG concentration. Additionally, increasing  $Re$  and decreasing  $D_r$  enhanced fluid mixing.
- Co-axial injection in the horizontal section benefited from the reduction of  $C_i$ ,  $D_r$ , and an increase in  $Re$  to promote more efficient mixing. For all injection locations, lowering the Froude number ( $Fr$ ) consistently improved mixing.

This study sheds light on the complex interplay of injection parameters on MEG-water mixing and offers valuable insights for the oil and gas exploration industry. Future research may expand the range of parameters through CFD simulations, providing guidance for planning experiments in large-scale geometries more representative of real-world applications in the field of oil and gas exploration.

#### 5. REFERENCES

- Akbari, S.; Taghavi, S. M., 2020. Injection of a heavy fluid into a light fluid in a closed-end pipe. *Physics of Fluids*, v. 32, n. 6, p. 063302.
- Akbari, S.; Taghavi, S. M., 2021. Fluid experiments on the dump bailing method in the plug and abandonment of oil and gas wells. *Journal of Petroleum Science and Engineering*, v. 205, p. 108920.
- Alba, K. et al., 2013. Miscible density-unstable displacement flows in inclined tube. *Physics of Fluids*, v. 25, n. 6, p. 067101.
- Alef, K. et al., 2018. The effect of regenerated MEG on hydrate inhibition performance over multiple regeneration cycles. *Fuel*, v. 222, p. 638-647.
- Alharooni, K. et al., 2015. Inhibition effects of thermally degraded MEG on hydrate formation for gas systems. *Journal of Petroleum Science and Engineering*, v. 135, p. 608-617.
- Aminnaji, M. et al., 2017. Effect of injected chemical density on hydrate blockage removal in vertical pipes: Use of MEG/MeOH mixture to remove hydrate blockage. *Journal of Natural Gas Science and Engineering*, v. 45, p. 840-847.
- Amiri, A. et al., 2016. Buoyant miscible displacement flows in vertical pipe. *Physics of Fluids*, v. 28, n. 10, p. 102105.
- Burgass, R., Chapoy, A., Li, X., 2018. Gas hydrate equilibria in the presence of monoethylene glycol, sodium chloride and sodium bromide at pressures up to 150 MPa. *The Journal of Chemical Thermodynamics*, v. 118, p. 193-197.
- Etrati, A. et al., 2018. Two-layer displacement flow of miscible fluids with viscosity ratio: Experiments. *Physics of Fluids*, v. 30, n. 5, p. 052103.

- Hassanzadeh, H. et al., 2021. Positively buoyant jets: semiturbulent to fully turbulent regimes. *Physical Review Fluids*, v. 6, n. 5, p. 054501.
- Karami, H., Pereyra, E., Sarica, C., 2017. Effects of monoethylene glycol (MEG) on three-phase flow characteristics in near-horizontal pipes. *Journal of Petroleum Science and Engineering*, v. 149, p. 834-843.
- Keulegan, G. H. Interfacial instability and mixing in stratified flows. US Department of Commerce, National Bureau of Standards, vol. 43, 1949.
- Najibi, H. et al., 2022. Natural gas hydrate stability conditions and water activity in aqueous solutions containing monoethylene glycol (MEG) and salt: Experimental measurements and thermodynamic modeling. *Fluid Phase Equilibria*, v. 554, p. 113322.
- Sahu, K. C. et al., 2009. Pressure-driven miscible two-fluid channel flow with density gradients. *Physics of Fluids*, v. 21, n. 4, p. 043603.
- Valim, L.S., 2018. Simulação fluidodinâmica da mistura de correntes líquidas aplicada à injeção de inibidores termodinâmicos de hidratos de gás. Masters thesis, Universidade Federal do Rio de Janeiro, Rio de Janeiro, Brasil.
- Wang, Y. et al., 2019. Hydrate formation management simulations with anti-agglomerants and thermodynamic inhibitors in a subsea tieback. *Fuel*, v. 252, p. 458-468.

## **6. RESPONSIBILITY NOTICE**

The authors are the only responsible for the printed material included in this paper.